Research Article

Gianfranco Spavieri and Espen Gaarder Haug*

The reciprocal linear effect, a new optical effect of the Sagnac type

Abstract: The Sagnac effect can be demonstrated with light propagating either along a circular contour or, as done by Wang *et al.*, back and forth along a linear contour. In the linear Sagnac effect, the emitter–receiver device is in motion relative to the contour where light propagates. In the reciprocal linear Sagnac effect (RLSE), the device is stationary and the contour is in motion. When the contour changes direction of motion, some special features of the linear Sagnac effect are not fully reciprocal to the RLSE, which foresees variations of the first order in v/c in the round-trip time taken by a light signal to cover the contour. The RLSE can be tested with present technology and, if confirmed experimentally, it might have interesting technological applications. Presently, it can be important for testing light-speed invariance, simultaneity, and the relativity principle.

Keywords: light propagation, Sagnac effect, one-way speed of light, relative simultaneity, Lorentz invariance

1 Introduction

The experiment related to the circular Sagnac effect [1], shown in Figure 1(a), was performed in 1913, and the one corresponding to the linear effect, shown in Figure 1(b), was accomplished by Wang *et al.* [2] in 2003. In both effects, the measuring device C* (emitter–receiver clock or interferometer) is in motion relative to a stationary contour, and C* measures the difference ΔT of the round-trip times of two light signals counterpropagating around the contour. Following Post [3], ΔT is given by,

* Corresponding author: Espen Gaarder Haug, Norwegian University of Life Sciences, Christian Magnus Falsensvei 18, 1433 As, Norway, e-mail: espenhaug@mac.com

Gianfranco Spavieri: Centro de Fiiisica Fundamental, Universidad de Los Andes, Mérida, 5101, Venezuela, e-mail: gspavieri@gmail.com

$$\Delta T = T_{\Leftarrow} - T_{\Rightarrow}$$
$$= \frac{2L}{\gamma(c - v)} - \frac{2L}{\gamma(c + v)} \qquad (1)$$
$$= \frac{4\gamma vL}{c^2} = \frac{2\gamma vP}{c^2},$$

where $T_{\Leftarrow}$ and $T_{\Rightarrow}$ represent the round-trip time of the co- and counter-moving light signals (or photons) along the contour of perimeter $P = 2\pi r$ or $2L$ in the circular and linear effects, respectively. For the circular Sagnac effect, with $v = \omega r$, result (1) is usually expressed [3] as $\Delta T = 4\omega \cdot A/c^2$, where A is the area enclosed by the light path.

In the linear Sagnac effect of Figure 1(b), the arm AB of the contour is stationary and the measuring device C* is moving clockwise with uniform speed v along the contour, going from the lower to the upper section of the contour and vice versa. While sliding around the pulley of radius R during the short time η, the device C* changes the direction of motion at the pulley A (or B). Locally, the speed v of C* relative to the contour is always constant. In the linear experiment performed by Wang *et al.* [2], the device C* is always in uniform rectilinear motion on the lower contour section during the round-trip time $T \simeq T_{\Leftarrow} \simeq T_{\Rightarrow}$. Therefore, in this experiment, C* does not turn around the pulleys A or B. However, since the relative speed v between C* and the contour is constant, there is no reason to suppose that the result differs from the theoretical prediction (1) if C* turns around the pulley during the round-trip time T.

In Section 2, we consider the reciprocal linear Sagnac effect (RLSE), shown in Figure 2, where the device C* is stationary and the contour is in relative motion. We find that, for counter-propagating light signals, the same observable ΔT in (1) is foreseen in the RLSE and, thus, with regard to ΔT, the RLSE is reciprocal to the linear Sagnac effect.

Nevertheless, within the context of standard special relativity based on light speed invariance, there are observable features of the linear Sagnac effect that are not reciprocal to those of the RLSE. In fact, when in the interval $T_{\Rightarrow}$ (or $T_{\Leftarrow}$) the device C* turns around the pulley in the linear Sagnac effect of Figure 1(b), for the corresponding RLSE of Figure 2, the Lorentz transformations (LTs) foresee variations in the first order in v/c for the interval $T_{\Rightarrow}$ (or $T_{\Leftarrow}$),
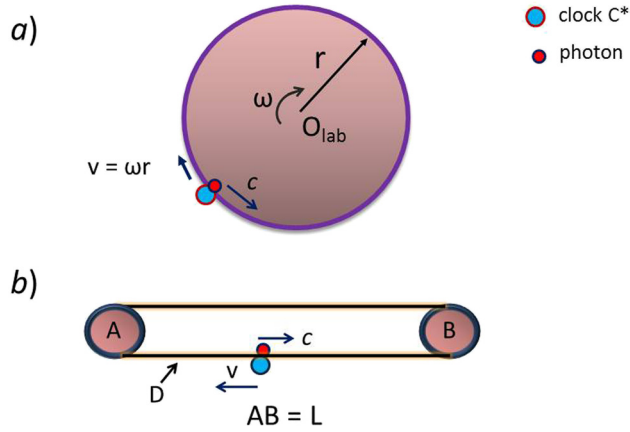
Figure 1: (a) In the circular Sagnac effect, two counter-propagating photons are emitted from the device C* and travel along the circumference of the rotating platform (only a single photon is shown). C* measures the difference ΔT of the arrival times after a round trip. (b) In the linear Sagnac effect, the counter-propagating photons travel in an optical fiber that may slide frictionless around the two pulleys A and B. The segment AC* of length D represents the initial position of device C* relative to A, the left end point of the contour. If AC* = $D > 2vL/c = (v/c)P$, the counter-moving photon performs a round trip and gets back to C* when this is still moving on the contour lower section.

which differ from that given by Eq. (1). Thus, if experimentally confirmed, the RLSE represents a new optical effect, which differs from the standard Sagnac effect.

In Section 3, we describe a realistic experiment, feasible with present technology, which can measure the mentioned variations related to the velocity v.
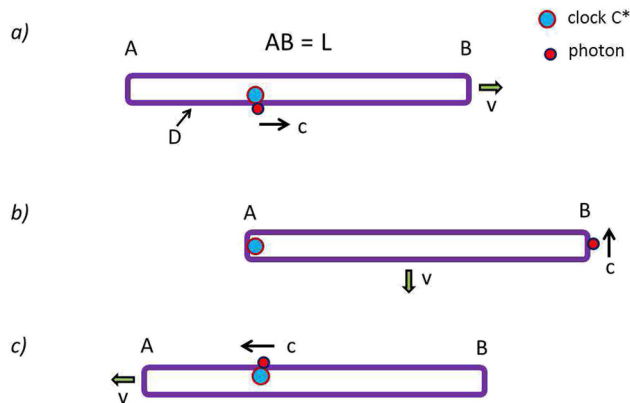

Figure 2: In the RLSE, the emitter–receiver C* is stationary and the contour of length ≈$2L = P$ is moving with a relative speed v. (a) The device C* emits a photon that travels on the contour lower section from the position AC* = $D < 2vL/c^2$. (b) When point A reaches C*, the contour changes direction of motion while sliding in the perpendicular direction at speed v on C* for a short negligible time interval η. (c) After the contour has resumed its motion in the horizontal direction, after a round-trip, C* receives the returning photon on the contour upper section.

There are no problems in interpreting the circular and linear Sagnac effect in the inertial frame of reference S_c of the stationary contour where the speed of light is assumed to be c, while different interpretations of the Sagnac effects are given [4–12] in the frame S_{C*} comoving with the device C*.

Some of the calculations that support our results are presented in the Appendix. Moreover, in the Appendix, we discuss some of the interpretations of the Sagnac effects in the wider scenario of relativistic theories [4–13], involving tests on simultaneity confirming that relative and absolute simultaneity are not physically equivalent. In this scenario, we show how the RLSE can be used as a test of light speed invariance.

2 The reciprocal linear Sagnac effect

In the RLSE of Figure 2, the measuring device C* (clock or interferometer) is stationary, while the whole contour is moving back and forth with uniform speed v relative to C*. Ideally, the motion of the contour should be such that, locally, the relative speed between the contour and C* would always be v. In Figure 2(a), the contour is moving with uniform motion relative to C*, which stays on the contour lower section until pulley A (not shown) reaches C*. At this moment, since C* is stationary, the contour has to move slightly in the direction perpendicular to AB during the short time η when sliding around C* at A, as shown in Figure 2(b). After changing direction of motion, the contour is moving relative to C*, now on the upper section as shown in Figure 2(c).

If the pulleys have diameter $2R$, the motion in the perpendicular direction $2H \simeq 2R$ takes place during the finite time interval $\eta \simeq \pi R/v$ when the contour is accelerating and changing its direction of motion relative to C*. However, for the purpose of simplifying calculations, we omit the process taking place during the negligible short finite interval η by assuming that the round-trip time T is much greater than η ($T \gg \eta$ and $L \gg \eta v \simeq 2H \simeq 2R$, while $(v/c)L \gg \eta c$). Thus, in the following, we consider the simple ideal case of a linear contour moving back and forth in the direction AB at the uniform speed v relative to C*. However, in the Appendix, we consider also the more realistic case of a rectangular contour where η is not negligible and the motion perpendicular to AB is taken into account.

Denoting by $P = 2L$ the perimeter of the contour, assuming the light speed to be c and using the LT, we find the following results valid for the RLSE:

(a) AC* = $D > 2vL/c = (v/c)P$. C* **remains always on one of the sections of the contour in the interval** T.

The segment AC* of length D represents the initial position of device C* relative to A, the left end point of the contour. For light counter-propagation (photon moving counter-clockwise) starting from the device C*, when $D > 2vL/c^2$ the description of the RLSE is reciprocal to that shown in (Figure 1(b)), where C* remains always on the lower section of the contour, while the photon performs a round trip in the interval $T_\Rightarrow$ and gets back to C*. The Lorentz-contracted moving contour has length L/γ and the round-trip times for counter-, $T_\Rightarrow$, and co-propagation, $T_\Leftarrow$, have the expected values,

$$T_\Rightarrow = \frac{2L}{\gamma(c+v)} = \frac{2\gamma L}{c}\left(1 - \frac{v}{c}\right)$$
$$T_\Leftarrow = \frac{2L}{\gamma(c-v)} = \frac{2\gamma L}{c}\left(1 + \frac{v}{c}\right) \tag{2}$$
$$\Delta T = T_\Leftarrow - T_\Rightarrow = \frac{4\gamma vL}{c^2} = \frac{4\gamma vL}{c^2} = \frac{2\gamma vP}{c^2},$$

where in Eq. (2), $T_\Leftarrow$, $T_\Rightarrow$, and ΔT are the same as given in Eq. (1). In some cases, we may approximate the results to the first order in v/c to simplify calculations. In Appendix (A.3), we calculate the round-trip interval $T_\Rightarrow$ for the counter-propagating photon emitted by C* from the distance AC* = $D > 2vL/c$, and show in (A15) that $T_\Rightarrow$ is independent of D when C* stays on the same track (lower contour section, in this case) during the interval $T_\Rightarrow$.

In this case ($D > 2vL/c$), the RLSE foresees results that are the same as those of the standard linear Sagnac effect. Moreover, the symmetry is such that $T_\Leftarrow$ is the same as $T_\Rightarrow$ by changing v to $-v$. It follows that, for AC* = $D > 2vL/c$, results (2) for the RLSE are equivalent to results (1) of the standard Sagnac effect. In fact, in agreement with the principle of relativity, provided that C* and the contour are in uniform relative motion in the interval $T_\Rightarrow$, the two effects are the same when observed either from the rest frame of the contour or the device C*.

(b) AC* = $D < 2vL/c$. C* **and the contour change their direction of relative motion in the interval** T.

In this case, for light counter-propagation, the successive positions of the contour relative to C* are shown in Figure 2, indicating that C* and the contour change their direction of relative motion during the round-trip time.

Special case $D = D_0 = vL/c$. Starting from D_0/γ (where the factor γ takes into account the length contraction of the moving contour) on the lower section of the contour, the photon travels at speed c toward the moving point B that, at time t, is at the distance $L/\gamma - D_0/\gamma + vt = (L/\gamma)(1 - v/c) + vt$. Then, the signal reaches point B when $ct = (L/\gamma)(1 - v/c) + vt$, i.e., after the time interval $t_{out} = L/(\gamma c)$. Moreover, since point

A is moving toward C* at speed v from the initial distance AC* = D_0, point A reaches C* when $vt = D_0/\gamma = vL/(\gamma c)$, i.e., at $t_{out} = L/(\gamma c)$. Hence, the two events "photon at B" and "A at the position of C*" are simultaneous in the reference frame S_{C^*} where C* is at rest, as shown in Figure 2(b). The return time interval of the photon from B to C* on the contour upper section is obviously $t_{ret} = L/(\gamma c)$, the return interval t_{ret} being independent of the motion of the contour. Then, in the RLSE of Figure 2(b), the return interval t_{ret} is the same regardless of whether the contour keeps moving to the right or starts moving to the left of the stationary C*.

Working out the calculations also for the co-propagating signal, for $T_\Leftarrow$, we find the exact result (A18) of Appendix (A.3). Then,

$$T_\Leftarrow = \frac{2L}{\gamma c} + \frac{4\gamma vL}{c^2}, \quad T_\Rightarrow = \frac{2L}{\gamma c}$$
$$\Delta T_{RLSE} = T_\Leftarrow - T_\Rightarrow = \frac{4\gamma vL}{c^2} = \frac{2\gamma vP}{c^2} \tag{3}$$
$$= \Delta T = \text{invariant.}$$

We see that, in the special case considered earlier where C* is initially on the lower and then on the upper section of the moving contour, the round-trip time $T_\Rightarrow$ in Eq. (3) is greater than the corresponding value in Eq. (2). However, also the round-trip time $T_\Leftarrow$ turns out to be greater than the corresponding value in (2). Then, for counter-propagating light signals, the difference ΔT_{RLSE} in Eq. (3) is still the same as in Eq. (2) and, as far as ΔT is concerned, $\Delta T = \Delta T_{RLSE} = $ invariant and the RLSE is equivalent to the standard linear Sagnac effect.

Special features of the RLSE. The important interesting feature of the RLSE is that in Eq. (3) the round-trip time $T_\Rightarrow$ of a single photon (i.e., the counter-propagating one) differs from the corresponding $T_\Rightarrow$ in Eq. (2). The difference persists as long as $0 < D < 2vL/c$ and C* moves from the lower to the upper section during the round-trip time $T_\Rightarrow$. Then, the function $T_\Rightarrow = T_\Rightarrow(D)$ varies from the minimum value given in Eq. (2) (for $D = 0$ or $D > 2vL/c$) to the maximum one given in Eq. (3) (for $D = D_0 = vL/c$). We must stress that $T_\Rightarrow$ is an observable measurable by clock C* and, for the standard linear Sagnac effect, the theory foresees $T_\Rightarrow = 2L/\gamma(c+v)$, independent of the value of D. Analogous considerations can be made for $T_\Leftarrow$.

Thus, results (2) and (3) indicate that there are special features of the RLSE not equivalent to those of the standard Sagnac effect. In case (b), when velocity variations are involved and C* and the contour change their direction of relative motion in the interval T, the differences indicate that the relativity principle does not hold. The differences between the two effects are interpreted below in the context of special relativity and the LT, showing that can be linked to relative simultaneity.

Since the standard RLSE, where $\Delta T = T_{\Leftarrow} - T_{\Rightarrow}$ is measured, is equivalent to the standard linear Sagnac effect, the usual approach based on measuring $\Delta T = \Delta T_{\text{RLSE}}$ = invariant does not reveal the special features of the RLSE. Then, for the purpose of pointing out these special features foreseen by the LT, we consider below the special reciprocal linear Sagnac effect (S-RLSE), and show how the S-RLSE can be tested and represents an optical effect with properties that differ from those of the standard linear Sagnac effect.

Testing the S-RLSE with an experiment

We pointed out that the round-trip $T_{\Rightarrow}$ of the counter-propagating signal is an observable that can be measured by the single clock C*. Therefore, the special features of the RLSE can be revealed with this type of measurements. In general, for precise measurements, we need to compare the observable $T_{\Rightarrow}$ with the corresponding observable T^* of a signal on a different light path. In the case of the S-RLSE, for the optical light path of the co-propagating photon, we choose a contour with the same perimeter $P = 2L$, but stationary in the device frame S_{C^*}.

Hence, the main difference between the RLSE and the S-RLSE is that in the RLSE, we have $T^* = T_{\Leftarrow}$, while in the S-RLSE, the round-trip time interval of the co-propagating signal is now $T^* = 2L/c$. With our choice, by means of (1), for the standard Sagnac effect, we have $\Delta T^*_{\text{Sagnac}} = T^* - T_{\Rightarrow} = 2L/c - 2\gamma(L/c)(1 + v/c) \simeq \Delta^*_{\text{Sagn}} = 2vL/c^2$ constant and independent of D. Instead, for the S-RLSE, we have $\Delta T^* = \Delta T^*(D) = T^* - T_{\Rightarrow} = T^* - T_{\Rightarrow}(D)$ dependent on D.

With the help of (2) and (3), we find,

$$D \gtrsim \frac{2vL}{c} \Rightarrow$$

$$\Delta T^*(D) = T^* - T_{\Rightarrow} = \frac{2L}{c} - \frac{2\gamma L(1 - v/c)}{c}$$

$$\simeq \frac{2vL}{c^2} = \Delta T^*_{\text{Sagnac}} = \Delta^*_{\text{Sagn}} \qquad (4)$$

$$D = D_0 \simeq \frac{vL}{c} \lesssim \frac{2vL}{c} \Rightarrow$$

$$\Delta T^*(D_0) = T^* - T_{\Rightarrow}(D_0) \simeq \frac{2L}{c} - \frac{2L}{c} = 0.$$

According to results (4), the function $\Delta T^*(D)$ is constant for $D \gtrsim 2vL/c$ and given by $2vL/c^2 = \Delta^*_{\text{Sagn}} = \Delta T^*_{\text{Sagnac}}$, which is the same for the RLSE and the linear Sagnac effect. However, for $D \lesssim 2vL/c$, the function $\Delta T^*(D)$ varies from the maximum values $2vL/c^2$ ($D = 0$ and $D = 2vL/c$) to zero ($D = D_0 = vL/c$), as shown in Figure 4. Analogous results, given in the following section and in the Appendix, are obtained when light propagates in a medium of refractive index n.

Thus, by assuming light speed invariance and the LT, the S-RLSE foresees the variant $\Delta T^*(D)$ of (4) that can be observed. The variant special feature of (4) is discussed in the Appendix within the wider scenario of relativistic theories. To fully understand the difference between the D-dependent S-RLSE results (4) and the D-independent results of the linear Sagnac effect in Eq. (2) and in Eq. (1), we consider the following corresponding interpretations.

2.1 Interpreting the RLSE and the linear Sagnac effect using the LTs

In the linear Sagnac effect and in the RLSE, the measurements are made by device C*. Why are the round-trip time intervals of the propagating signals different in the two effects? Let us, then, consider an observer comoving with clock C* (let us call it "observer C*" or simply "C*") and check first what happens in the linear Sagnac effect of Figure 1(b) when C* is near point A and, during the round-trip interval $T_{\Rightarrow}$, changes the direction of motion in the negligible time interval η moving from the lower to the upper section of the contour. While on the lower section, C* is comoving with the inertial frame S'' and with the inertial frame S' when on the upper section.

If the counter-propagating photon is emitted by C* at $AC^* = D_0 = (v/c)L$ when in the lower section frame S'', C* reaches A when, simultaneously, the photon reaches point B, as shown in Figure 3. Then, for the relative position of photon and C*, the situation is the same as that in the RLSE of Figure 2(b).

However, when (after reaching A and turning around the pulley) C* starts comoving with frame S' on the upper section, we can see in Figure 3 that now the position of the photon is not at B, but at K, being $AK \simeq L(1 - 2v/c) < L$ and, thus, the situation differs from that of Figure 2(b) of the RLSE.

The difference is due to the fact that, in the linear Sagnac effect, the mechanism of relative simultaneity takes place when C* changes velocity by moving from frame S'' on the lower section to the frame S' on the upper section [7]. The two events, "C* at A" and "photon at B," are simultaneous for observer C* on frame S'' in the lower section, but no longer simultaneous for C* on frame S' in the upper section because S' is in motion with speed $\simeq 2v$ relative to S''.

As shown in Figure 3, in the linear Sagnac effect, clock C* is reached by the photon returning on the upper section after the proper time interval $\tau_{\text{ret}} \simeq (L/c)(1 - 2v/c)$ and the round-trip time interval is, as expected, $(T_{\Rightarrow})_{\text{Sagnac}} = \tau_{\text{out}} + \tau_{\text{ret}} \simeq L/c + (L/c)(1 - 2v/c) = 2L/(c + v)$. In this case, relative to C*, in the return trip, the photon covers at speed c the shorter distance $L(1 - 2v/c)$ only.

However, in the case of the RLSE (Figure 2(b)), C* is stationary and, since the mechanism of relative simultaneity does not apply, in the return trip, the photon covers at speed c the full distance $\simeq L$ in the time interval $t_{\text{ret}} = L/(\gamma c) \simeq L/c$. Thus, for the special case $D = D_0 = vL/c^2$, in the RLSE, the round-trip time is $(T_{\Rightarrow})_{\text{RLSE}} \simeq 2L/c$, which is greater than the corresponding one $(T_{\Rightarrow})_{\text{Sagnac}} \simeq 2L/(c+v)$ of the linear Sagnac effect.

As shown in ref. [7], in the case of the linear Sagnac effect, the "time gap" $\delta t \simeq 2vL/c^2$, due to relative simultaneity between S' and S'', corresponds to the length difference $c\delta t \simeq 2vL/c$ not covered by the photon when C* is on the upper section. Therefore, we find that $(T_{\Rightarrow})_{\text{RLSE}} \simeq (T_{\Rightarrow})_{\text{Sagnac}} + \delta t$, showing that the difference can be related to relative simultaneity.

In general, in the linear Sagnac effect, the round-trip time T of light signals is independent of D and the stationary contour shape, while in the RLSE, the round-trip time T depends on D and on the shape of the moving contour. Then, the RLSE represents an optical effect not fully equivalent to the linear Sagnac effect.

3 Experiment testing the S-RLSE

Here, we discuss the results obtained for the rectangular contour of Figure 4 (shown also in Figure A1 of the Appendix) of sizes L and H. With $H \simeq 2R$, where R is the radius of the pulley in the linear Sagnac effect, the shape of this contour represents more realistically the RLSE.

For the rectangular contour of Figure A1, we assume that the contour slides continuously at the local speed v relative to C*. This is a mechanical difficulty that, in principle, can be surmounted, although it increases the cost of the experiment in comparison to the standard Sagnac experiments. Actually, for the experiment, the rectangular contour can move relative to C* for a short distance, starting with C* on the lower section L and ending on the left side H, as shown in Figure A1. For the size of the contour to be manageable, it is convenient to have light propagating in an optical fiber with a high refractive index n. In this case, the round-trip time is increased to $T_{\Rightarrow} \simeq nP/c$.

In the case of light propagation in a medium, we have to distinguish the case when the medium is locally at rest along the contour from the case when the medium is locally at rest with C* and sliding along the contour. The speed of light in the moving medium is obtained from the standard relativistic velocity transformations. The results using the LT, derived in the Appendix (neglecting dispersion), are shown schematically below.

S-RLSE with medium locally at rest with the contour $P = 2L + 2H$

$$T^* = \frac{nP}{c}, \quad \Delta T^* \simeq n^2 \frac{v}{c}\frac{P}{c}, \quad \text{independent of } D$$
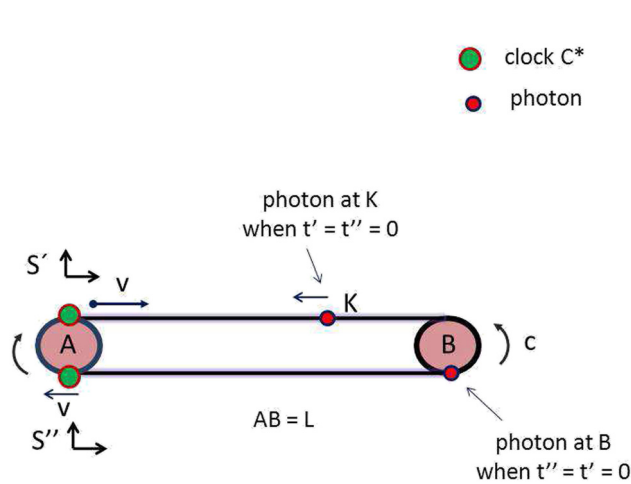

Figure 3: Effect of relative simultaneity observed by C* in the linear Sagnac effect. The two events "C* at A" and "photon at B" are simultaneous on frame S'' comoving with C* when on the contour lower section. After turning around the pulley in the negligible time interval η and changing velocity, C* starts comoving with frame S' on the upper section at $t' = t'' = 0$. However, due to relative simultaneity between S' and S'', for observer C* on S', the photon is no longer at B but is at K already.
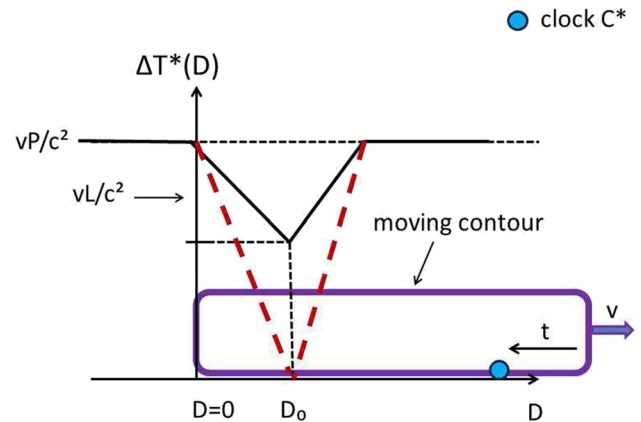

Figure 4: Time difference $\Delta T^*(D)$ for the counter-moving photon in the S-RLSE. For the Sagnac effect, $\Delta T^* = vP/c^2$ is constant and represented by the dotted line. For the S-RLSE, starting from right to left with C* on the contour lower section L from the position $D > 2vL/c^2$, we have $\Delta T^* = vP/c^2$ until $D = 2vL/c$. When $D < 2vL/c$ and until $D = D_0 = vL/c$, $\Delta T^*(D)$ decreases up to vL/c^2. Then, ΔT^* increases and reaches again the value vP/c^2 at $D = 0$ and afterwards when C* is on the left side H of the moving contour. The broken line refers to the S-RLSE of Figure 2, where $P = 2L$ and the dip is $2vL/c^2$ with $\Delta T^* = 0$ at $D = D_0$.

$$D = D_0 \simeq \frac{vnL}{c^2}, \quad T_\Rightarrow \simeq \frac{nP}{c} - n^2\frac{v}{c}\frac{P}{c} + \frac{vL}{c^2}$$

$$D = D_0 \simeq \frac{vnL}{c^2}, \quad \Delta T^*(D_0) = T^* - T_\Rightarrow \simeq \Delta^*_{\mathrm{Sagn}} - \frac{vL}{c^2}$$

$$D > \frac{2vnL}{c^2}, \quad T_\Rightarrow \simeq \frac{nP}{c} - n^2\frac{v}{c}\frac{P}{c}$$

$$D > \frac{2vnL}{c^2}, \quad \Delta T^*(D) = T^* - T_\Rightarrow \simeq \Delta^*_{\mathrm{Sagn}}. \tag{5}$$

S-RLSE with medium locally
at rest with C*, $P = 2L + 2H$

$$T^* = \frac{nP}{c}, \quad \Delta^*_{\mathrm{Sagn}} \simeq \frac{v}{c}\frac{P}{c}, \quad \text{independent of } D$$

$$D = D_0 \simeq \frac{vnL}{c^2}, \quad T_\Rightarrow \simeq \frac{nP}{c} - \frac{v}{c}\frac{P}{c} + \frac{vL}{c^2}$$

$$D = D_0 \simeq \frac{vnL}{c^2}, \quad \Delta T^*(D_0) = T^* - T_\Rightarrow \simeq \Delta^*_{\mathrm{Sagn}} - \frac{vL}{c^2}$$

$$D > \frac{2vnL}{c^2}, \quad T_\Rightarrow \simeq \frac{nP}{c} - \frac{v}{c}\frac{P}{c}$$

$$D > \frac{2vnL}{c^2}, \quad \Delta T^*(D) = T^* - T_\Rightarrow \simeq \Delta^*_{\mathrm{Sagn}}. \tag{6}$$

For the S-RLSE with medium locally at rest with device C*, Figure 4 shows $\Delta T^* = \Delta T^*(D)$ as a function of D. For the Sagnac effect, $\Delta T^* = \Delta T^*_{\mathrm{Sagnac}} = \Delta^*_{\mathrm{Sagn}} = vP/c^2$ is constant. For the S-RLSE, $\Delta T^*(D)$ is represented by the solid line that varies as a function of the initial position D of clock C*. For the S-RLSE, the LT foresee, the observable dip by vL/c^2 in the function $\Delta T^*(D)$. The broken line refers to the S-RLSE of Figure 2, where $P = 2L$ and the dip is $2vL/c^2$ with $\Delta T^* = 0$ at $D = D_0$.

Expected precision for the S-RLSE

The variation $\Delta T^*(D)$ may be measured with the techniques of ring interferometry or, after some adaptations, ring lasers [3]. Ring lasers Sagnac experiments, which can measure the angular velocity ω_E of the Earth with a precision $\delta\omega/\omega_E < 10^{-8}$, are performed routinely on the Earth [14,15]. For the effect of refractive index of an optical medium on the rotation frequency of ring lasers and resonators, there are various experimental expressions as functions of n, considered by Malykin in ref [16] (2014).

In relation to the sensitivity of detectors measuring $\delta\tau_A$ and the smallest measurable time interval, there are techniques capable of resolving femtosecond (10^{-15} s) [17] or even attosecond (10^{-18} s) [18] pulses of laser light, although better limits may be obtained by means of advanced interferometry.

The dip by vL/c^2, to be measured to confirm the prediction of standard relativity based on the LT, is comparable to that measured in the usual experiments testing the Sagnac effect and, thus, well within the range of the sensitivity of available detectors and not too difficult to observe.

In the experiment by Wang et al. [2], the device C* is in motion relative to the contour. In the S-RLSE, the device C* is stationary and the contour in relative motion. Assuming the same relative velocity, we expect that the sensitivity achievable for our S-RLSE experiment is approximately the same as that achieved in the experiment by Wang et al. [2]. The main difference with respect to the experiment by Wang et al. is related to the mechanical difficulties involved with the motion of the contour, which implies more an increase in the complexity and cost of the experiment, rather than a loss in sensitivity.

Possible applications of the S-RLSE if confirmed experimentally.

After more than a century, the Sagnac effect is employed in current technology and is used in inertial guidance systems, ring laser gyroscope (extremely sensitive to rotations), and other optical systems. Being not yet experimentally confirmed, it might be premature to indicate what kind of applications the RLSE might have. However, considering that the circular Sagnac effect (sensitive to rotations) can detect very accurately the angular velocity of objects, such as the Earth, the RLSE (sensitive to velocity changes) might be suitable to detect velocity variations and also point out the corresponding direction. The realization of these applications requires, however, to take into account other features related to the RLSE that will be considered in a future contribution.

4 Conclusions

We have described an optical effect, denoted as RLSE, where the emitter–receiver device is stationary and the contour along which light propagates is in motion. The RLSE provides the same results of the standard Sagnac effect for the round-trip time difference ΔT of light signals counter-propagating along the closed contour. However, the RLSE possesses features that are not equivalent to the corresponding ones of the Sagnac effect. When the contour changes velocity, standard special relativity foresees that the round-trip time interval $T_\Rightarrow$ of a counter-moving light signal differs from the corresponding one of the Sagnac effect. The difference is observable with our S-RLSE experiment and given by the dip by vL/c^2 in the measured round-trip time difference $\Delta T^*(D) = T^* - T_\Rightarrow$ of counter-propagating photons, plotted in Figure 4. The dip may be related to the different role played by relative simultaneity in the linear Sagnac effect and the RLSE.

If confirmed experimentally, the S-RLSE stands to be a new relativistic optical effect. In this case, being sensitive to velocity changes, the S-RLSE might have important

technological applications in inertial guidance systems by detecting velocity variations and corresponding direction.

In any event, the different features between the standard linear Sagnac effect and the S-RLSE can be exploited for testing Lorentz and light speed invariance.

Author contributions: All authors have accepted responsibility for the entire content of this manuscript and approved its submission.

Conflict of interest: The authors state no conflict of interest.

References

[1] Sagnac G. Regarding the proof for the existence of a luminiferous ether using a rotating interferometer experiment. C R Acad Sci. 1913;157:708–10.

[2] Wang R, Zhengb Y, Yao A, Langley D. Modified Sagnac experiment for measuring travel-time difference between counter-propagating light beams in a uniformly moving fiber. Phys Lett A. 2003;312:7–10. Wang R, Zheng Y, Yao A. Generalized Sagnac effect. Phys Rev Lett. 2004;93(14):143901.

[3] Post EJ. Sagnac effect. Rev Mod Phys. 1967;39(2):475–93.

[4] Lee C. Simultaneity in cylindrical spacetime. Am J Phys. 2020;88:131.

[5] Klauber RD. Comments regarding recent articles on relativistically rotating frames. Am J Phys. 1999;67(2):158–9.

[6] Selleri F. Noninvariant one-way velocity of light. Found Phys. 1996;26:641. Noninvariant one-way speed of light and locally equivalent reference frames. Found Phys Lett. 1997;10:73–83.

[7] Spavieri G, Gillies GT, GaarderHaug E, Sanchez A. Light propagation and local speed in the linear Sagnac effect. J Modern Optics. 2019;66(21):2131–41. doi: 10.1080/09500340.2019.1695005. Spavieri G, Gillies GT, Gaarder Haug E. The Sagnac effect and the role of simultaneity in relativity theory. J Mod Opt. 2021. doi: 10.1080/09500340.2021.1887384. Spavieri G. On measuring the one-way speed of light. Eur Phys J D. 2012;66:76. doi: 10.1140/epjd/e2012-20524-8; Spavieri G. Light propagation on a moving closed contour and the role of simultaneity in special relativity. Eur J Appl Phys. 2021;3:4:48. doi :10.24018/ejphysics.2021.3.4.99; Spavieri G, Gaarder Haug E. Testing light speed invariance by measuring the one-way light speed on earth. Physics Open 2022;12:100113. doi: 10.1016/j.physo.2022.100113.

[8] Gift SJG. On the Selleri transformations: analysis of recent attempts by Kassner to resolve Selleri's paradox. Appl Phys Res. 2015;7(2):112.

[9] Kipreos ET, Balachandran RS. An approach to directly probe simultaneity. Modern Phys Lett A. 2016;31(26):1650157; Assessment of the relativistic rotational transformations. Modern Physics Letters A. 2021;36(16):2150113.

[10] Landau LD, Lifshitz EML. The classical theory of fields. Vol. 2. 2nd English edn. Pergamon Press; 1962. p. 236.

[11] Lundberg R. Critique of the Einstein clock variable. Phys essays. 2019;32:237; Travelling light. J Mod Opt. 2021;68(14). doi: 10.1080/09500340.2021.1945154.

[12] Field JH. The Sagnac effect and transformations of relative velocities between inertial frames. Fund J Modern Phys. 2017;10(1):1–30.

[13] Mansouri R, Sexl RU. A test theory of special relativity: I. Simultaneity and clock synchronization. Gen Rel Grav. 1977;8:497, 515, 809.

[14] Schreiber KU, Gebauer A, Igel H, Wassermann J, Hurst RB, Wells JPR. The centennial of the Sagnac experiment in the optical regime: from a tabletop experiment to the variation of the Earth's rotation. C R Physique. 2014;15:859–65. doi: http://dx.doi.org/10.1016/j.crhy.2014.10.003.

[15] Stedman GE. Ring-laser tests of fundamental physics and geophysics. Rep Prog Phys. 1997;60:615.

[16] Malykin GB. The Sagnac effect: correct and incorrect explanations. Phys Uspekhi. 2000;43(12):1229–52.

[17] Ludlow DA, Boyd MM, Ye J, Peik E, Schmidt PO. Optical atomic clocks. Rev Mod Phys. 2015;87:637.

[18] Kim J, Chen J, Cox J, Kärtner FX. Attosecond-resolution timing jitter characterization of free-running mode-locked lasers. Optics Lett. 2007;32(24):3519–21; Kwon D, Jeon CG, Shin J, Heo MS, Park SE, Song Y, Kim J. Ultrafast, subnanometre-precision and multifunctional time-of-flight detection. Scientific Reports 2017;7:40917.

[19] Tangherlini FR. An introduction to the general theory of relativity. Nuovo Cimento Suppl. 1961;20:1.

[20] Spavieri G, Rodriguez M, Sanchez A. Thought experiment discriminating special relativity from preferred frame theories. J Phys Commun. 2018;2:085009. doi: 10.1088/2399-6528/aad5fa.

[21] de AbreuR, Guerra V. On the consistency between the assumption of a special system of reference and special relativity. Found Phys. 2006;36:1826–45.

[22] Bell JS. Speakable and unspeakable in quantum mechanics. Cambridge: Cambridge University Press; 1988.

[23] Anderson R, Vetharaniam I, Stedman GE. Conventionality of synchronisation, gauge dependence and test theories of relativity. Phys Rep. 1998;295:93–180.

[24] Popper K. Conjectures and refutations. London: Routledge; 1963; Kuhn TS, The structure of scientific revolutions. Chicago, Illinois: University of Chicago Press; 1962.

[25] Eisele C, Nevsky AY, Schiller S. Laboratory test of the isotropy of light propagation at the 10^{17} level. Phys Rev Lett. 2009;103:090401.

[26] Hughes VW, Robinson HG, Beltran-Lopez V. Upper limit for the anisotropy of inertial mass from nuclear resonance experiments. Phys Rev Lett. 1960;4:342–4.

[27] Drever RWP. A search for anisotropy of inertial mass using a free precession technique. Phil Mag. 1961;6:683–7.

[28] Pruttivarasin T, Ramm M, Porsev SG, Tupitsyn II, Safronova MS, Hohensee MA, et al. Häffner H. Michelson-Morley analogue for electrons using trapped ions to test Lorentz symmetry. Nature. 2015;517:592–5. doi: 10.1038/nature14091.

[29] Thomas LH. The motion of the spinning electron. Nature (London). 1926;117:514; The kinematics of an electron with an axis. Phil Mag. 1927;3:1–22.

[30] Jackson JD. Classical Electrodynamics, Sect. 11.8. 2nd edn. New York: John Wiley & Sons, Inc; 1975.

[31] Bargmann V, Michel L, Telegdi VL. Precession of the polarization of particles moving in a homogeneous electromagnetic field. Phys Rev Lett. 1959;2:435.

Appendix

A.1 Special reciprocal linear Sagnac effect for light propagation in a medium of refracting index n on a rectangular contour of sides L and H

For the S-RLSE, the round-trip interval $T_\Rightarrow$ differs from the corresponding one of the linear Sagnac effect if, on the contour lower section, to the first order in v/c, $D \simeq nvL/c$ and the photon reaches the right corner when the left corner reaches C*.

S-RLSE with medium locally at rest with the contour. $P = 2L + 2H$.

For the contour of Figure A1(a), we calculate with the LT to the first order in v/c the time intervals taken by the counter-propagating photon to cover the sides of the rectangular contour in motion with velocity v relative to the stationary C*.

Position 1: Starting from $D = vt \simeq nvL/c$, and using the equation $C_n t = L - D + vt$ with C_n the light speed relative to C*. Then, we have,

$$C_n = \frac{c/n + v}{1 + v/nc}$$

$$t_1 = \frac{L}{C_n} = \frac{nL(1 + v/nc)}{c(1 + nv/c)} \simeq \frac{nL}{c} - \frac{n^2 vL}{c^2} + \frac{vL}{c^2}.$$

Position 2: By means of the equation $C_n t = H - vt$,

$$C_n = \frac{c/n - v}{1 - v/nc}$$

$$t_2 = \frac{H}{C_n + v} \simeq \frac{nH(1 - v/nc)}{c} \simeq \frac{nH}{c} - \frac{vH}{c^2}.$$

Position 3: With the equation $C_n t = L$,

$$C_n \simeq \frac{c}{n}$$

$$t_3 = \frac{L}{C_n} \simeq \frac{nL}{c}.$$

Position 4: By means of the equation, $C_n t = H - v(t_2 + t_3)$,

$$C_n = \frac{c/n + v}{1 + v/nc}$$

$$t_4 = \frac{nH(1 + v/nc)}{c(1 + nv/c)} - \frac{n^2 vH}{c^2} - \frac{n^2 vL}{c^2}$$

$$= \frac{nH}{c} - \frac{n^2 vH}{c^2} + \frac{vH}{c^2} - \frac{n^2 vH}{c^2} - \frac{n^2 vL}{c^2}$$

$$T_\Rightarrow = t_1 + t_2 + t_3 + t_4 = \frac{nP}{c} - n^2 \frac{v}{c} \frac{P}{c} + \frac{vL}{c^2}.$$

S-RLSE medium locally at rest with the device C*. $P = 2L + 2H$.

For the contour of Figure A1(b), we calculate with the LT to the first order in v/c the time intervals taken by the counter-propagating photon to cover the optical fiber sliding on the moving rectangular contour.

Position 1: Starting from $D = vt$, by means of the equation $C_n t = L - D + vt$ with C_n the light speed relative to C* along the fiber at rest, we have,

$$C_n = \frac{c}{n}$$

$$t_1 = \frac{L}{C_n} = \frac{nL}{c}.$$

Position 2: From the equation $C_n t = H - vt$ and with the optical fiber at speed $2v$ relative to C*,

$$C_n = \frac{c/n - 2v}{1 - 2v/nc}$$

$$t_2 = \frac{H}{C_n + v} \simeq \frac{nH(1 - 2v/nc)}{c(1 - nv/c)}$$

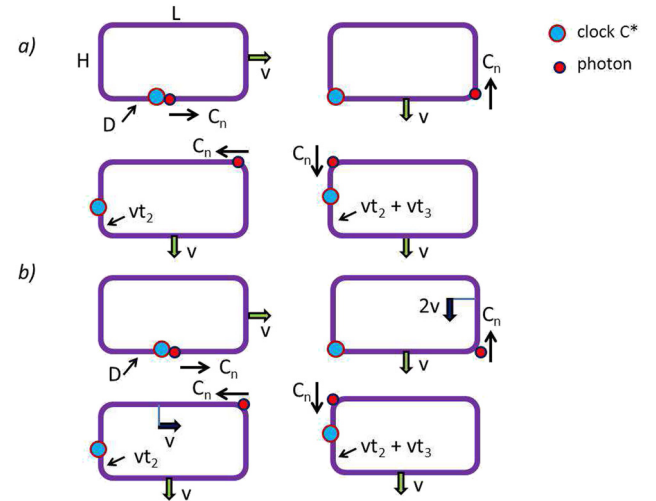$$\simeq \frac{nH}{c} + \frac{n^2 vH}{c^2} - \frac{2vH}{c^2}.$$

Figure A1: (a) Optical fiber of index n locally at rest on the rectangular contour moving with velocity v relative to the stationary clock C*. The photon starts from C* at the distance D from the contour left side H and returns to C* in the interval $T_\Rightarrow$ after traveling along the contour sides at different speeds C_n relative to C*. (b) Optical fiber of index n locally at rest with C* and sliding on the rectangular contour moving with velocity v relative to the stationary clock C*. In position 1, the fiber in the lower contour section is at rest relative to C*. In 2, the sliding fiber has speed $2v$ relative to C*. In 3, the relative speed is v and in 4, the fiber is at rest relative to C*.

Position 3: By means of the equation $C_n t = L$ and with the optical fiber at speed v,

$$C_n \simeq \frac{c/n - v}{1 - v/nc}$$

$$t_3 = \frac{L}{C_n} = \frac{nL(1 - v/nc)}{c(1 - nv/c)}$$

$$\simeq \frac{nL}{c} + \frac{n^2 vL}{c^2} - \frac{vL}{c^2}.$$

Position 4: From the equation $C_n t = H - v(t_2 + t_3)$ and with the optical fiber at rest,

$$C_n = \frac{c}{n} t_4 = \frac{nH}{c} - \frac{n^2 vH}{c^2} - \frac{n^2 vL}{c^2}$$

$$T_\rightarrow = t_1 + t_2 + t_3 + t_4 = \frac{P}{c}\left(n - \frac{v}{c}\right) + \frac{vL}{c^2}.$$

A.2 Interpreting optical effects and the RLSE in the scenario of relativistic theories

Several authors [4,13,19–23] argue that the LT are physically equivalent to alternative coordinate transformations that differ from the LT by an arbitrary clock synchronization parameter only. Thus, these authors claim that the one-way light speed is undetermined, or conventional, when measured by two spatially separated clocks that can be arbitrarily synchronized. In the framework of relativistic theories [13], the coordinate transformations alternative to the LT, more often used to describe physical phenomena, are denoted as LTs based on absolute simultaneity (LTA). The LT and the LTA are expressed as,

$$\begin{array}{ll} LT & t' = \gamma(t - vx/c^2) \quad x' = \gamma(x - vt) \\ LTA & t' = t/\gamma \quad x' = \gamma(x - vt), \end{array} \tag{A1}$$

where in (A1) v indicates the velocity of frame S' relative to frame S and the transformations $y' = y$; $z' = z$ are understood. With the factor $\gamma = (1 - v^2/c^2)^{-1/2}$ depending on v, LT stands for the LTs, based on standard synchrony and relative simultaneity. LTA stands for the LTs based on absolute synchrony and simultaneity. To the first order in v/c, the LTA coincides with the Galileo transformations. The LTA (or ALT in Ref. [9]) are known in literature also as the Tangherlini–Selleri transformations [6,19,20], used by several authors [4–9].

Because of the arbitrariness of synchronization and one-way light speed, many physicists consider the LT and LTA to be physically equivalent and, according to them, the LTA can be used to interpret all the experiments supporting standard special relativity [13,21–23]. Certainly, the equivalence should hold in the cases when the one-

way light speed is conventional because measured by two spatially separated clocks that are arbitrarily synchronized. However, in the Sagnac effects, the one-way speed of light around the contour can be determined with the single clock C* and no arbitrary clock synchronization is involved. Thus, in relation to the difficulties pointed out in the interpretations of the Sagnac effect [6–9,11], several authors [4–9] have shown that the difficulties are surmounted if, in lieu of the LT based on relative simultaneity, coordinate transformations based on conservation of simultaneity (LTA) are adopted.

Nevertheless, epistemologists [24] claim that the basic postulates of a meaningful physical theory must be testable (*i.e.*, falsifiable). Then, if one of its basic postulates is not falsifiable, it may be argued by physicists and epistemologists [24] that the theory is not physically meaningful. If the LT (with relative simultaneity) are equivalent to the LTA (with absolute simultaneity) and the speed of light is conventional, the *standard* theory of special relativity has a drawback because its fundamental postulate of one-way light speed invariance cannot be tested [13,19–23]. For this reason, in the more recent formulation of special relativity found in mainstream physics journals where light speed is conventional [4], the constant c in the second postulate is no longer the one-way light speed, but *"the round-trip speed of light (*i.e., *the average speed of light during the round-trip from A to B and then back to A),"* which is observable.

Nevertheless, *standard* special relativity is based on the LT and, for determining the good standing of this theory and the LT, it is essential to establish whether the LTA and the LT are, or are not, physically equivalent.

It is worth mentioning that in practically all the experiments supporting special relativity what is being tested are effects related to relativistic time dilation and length contraction, equally foreseen by the LT and the LTA [4–9,13]. Special relativity is a very well tested theory confirmed by high precision experiments [13,25–28]. The experiments performed so far are likely suitable to test [13] the so-called relativistic effects only, which are of second (or higher) order in v/c and are not dedicated experiments capable of testing the special different features of the LT and LTA, relative versus absolute simultaneity, because these differences vanish on average. In literature, there are proposals of dedicated experiments of first order in v/c that might test the different features of simultaneity, relative or absolute (see, for example, [7,20]). However, up to now and as far as we know, no experiments of this type have been performed. Yet, as shown below, these different features can be tested by means of the RLSE also.

A.2.1 The LTA and LT foresee different results for the RLSE

In the interpretation of the optical effects of the Sagnac type with the LTA, we are looking for the preferred frame where the one-way light speed can be assumed to be c. The natural choice is given by the contour inertial rest frame S_c where Maxwell's equations are valid, and the electromagnetic waves, locked on the contour, propagate at speed c. With this choice of the preferred frame, from the contour inertial frame S_c, the LTA and LT provide an equivalent interpretation with the same results.

If, for the RLSE of Figure 2, we choose again the contour to be the preferred frame, then, we may assume that while moving with uniform velocity relative to C* the contour is carrying along the electromagnetic waves, always propagating at the local speed c relative to the contour. With the aforementioned assumptions, we find that in the framework of the LTA, the RLSE is fully reciprocal to the linear Sagnac effect. In fact, save for the negligible time interval η when the contour changes velocity, the observer S_c comoving with the contour of Figure 2 is on an inertial frame before and after the interval η. Then, as far as the RLSE is concerned, the result is independent of whether the relative change of motion is performed by C* or the contour. Since simultaneity is conserved with the LTA, when the contour changes velocity, there are no variations in the relative positions of photon and C*, unlike what happens with relative simultaneity in Figure 3. Therefore, if calculated from the contour frame S_c, the invariant proper time interval $T_\Rightarrow$ is the same as in the linear Sagnac effect. However, when calculated from clock frame S_{C*} we have to take into account that with the LTA light speed is no longer invariant.

To verify that, with the LTA, the invariant interval $T_\Rightarrow$ in the RLSE is independent of D and the same as in the linear Sagnac effect, we calculate it from the clock frame S_{C*} for the case when the contour changes velocity in the interval $T_\Rightarrow$, as in Figure 2. Let the photon start from C* at D and travel toward point B moving to the right (Figure 2(a)). Relative to C*, by addition of velocities, the light speed along the moving contour is $\approx c + v$, where for simplicity we use the first-order approximation in v/c. In the out trip and at time t, point B is at the position $L - D + vt$ to the right of C* and the photon reaches B when $(c + v)t = L - D + vt$. Considering first the special case when simultaneity takes place, we set $D = vt$ and, thus, $t = t_{out} = L/(c + v)$ and $D = vt_{out} \approx vL/c$. Then, the two events "photon at B" and "A at C*" are simultaneous in every frame. In the return trip on the upper section (Figure 2(b)), the contour is now moving to the left, while the photon travels on the upper section toward the stationary

C* at the speed $\approx c + v$. With the photon coming from B at L, the return time interval is $t_{ret} = L/(c + v)$ and the round-trip is $T_\Rightarrow = t_{out} + t_{ret} \approx 2L/(c + v)$, which is the same as in the linear Sagnac effect shown in (2).

It can be shown that the same result, independent of D, is obtained in general, *e.g.*, when the photon reaches B before A reaching C* (or when A reaches C* before the photon reaching B) and when C* is always on the lower (or upper) section of the contour in the round-trip interval $T_\Rightarrow$.

In conclusion, with the LTA based on absolute simultaneity, the RLSE is fully equivalent to the linear Sagnac effect and the relativity principle is holding. For the S-RLSE experiments described earlier, contrary to the LT, the LTA foresee that the variant (for the LT) function $\Delta T^*(D)$ is (for the LTA) always $\Delta T^* = \Delta T^*_{Sagnac}$, independent of D. It follows that, by means of the S-RLSE, the different predictions of the LT and LTA, and light speed invariance, can be tested.

Another example indicating that the LT and LTA are not equivalent, and cannot be arbitrarily interchanged in the description of physical phenomena, is given by the Thomas precession, discussed below.

A.2.2 Using the Thomas precession to discriminate relative (LT) from absolute (LTA) simultaneity

In the following, we consider the relativistic phenomenon of the Thomas precession [29] and find that it is predicted by the LT but not by the LTA. Since the spacetime symmetry of the LT differs from that of the LTA, it is not surprising that the two transformations predict different results. Standard special relativity is routinely used in several areas of modern physics employing the symmetry of the LTs based on relative simultaneity and the Thomas precession derived from the LT is well known for predicting the correct spin–orbit interaction energy splitting [29,30] and is thus considered to be observable. Moreover, Thomas' precession is included in the equation of spin motion of the BMT equation of elementary particle physics [31]. However, so far there are no direct tests of the Thomas precession.

Deriving the Thomas precession with the LT

Here, we consider the textbook derivation made by Jackson [30] and indicate schematically the steps that lead to the Thomas precession. In deriving the spin precession for the case of spin–orbit interaction, Thomas considers an electron orbiting on a plane at the peripheral velocity v around the nucleus of an atom. Thomas shows that, because of the motion of the electron in its circular orbit with the acceleration a due to the Coulomb field, the electron spin acquires an extra angular velocity ω_T of

purely relativistic kinematical origin. The Thomas angular velocity $\boldsymbol{\omega}_T$, corresponding to the rotation per unit of time of the electron frame, can be calculated from the infinitesimal LT along the electron path (shown in Figure A2), indicating that successive transformations consist of a pure boost and a rotation.

To point out the origin of the rotation of the particle rest frame S'', in his approach to the Thomas precession, Jackson starts from the LT between the two frames S'' and S given by (Ref. [30], Section 11.19),

$$
\begin{aligned}
x_0'' &= \gamma_u (x_0 - \boldsymbol{\beta} \cdot \mathbf{x}) = \gamma_u (x_0 - \beta_1 x_1 - \beta_2 x_2) \\
x_1'' &= x_1 + \frac{\gamma_u - 1}{\beta^2}(\beta_1 x_1 + \beta_2 x_2)\beta_1 - \gamma \beta_1 x_0 \\
x_2'' &= x_2 + \frac{\gamma_u - 1}{\beta^2}(\beta_1 x_1 + \beta_2 x_2)\beta_2 - \gamma \beta_2 x_0 \\
x_3'' &= x_3,
\end{aligned}
\tag{A2}
$$

where, as shown in Figure A2, S'' is in motion with velocity components $u_x = u_1$ and $u_y = u_2$ relative to the laboratory frame S and in (A2) $\gamma_u = (1 - u^2/c^2)^{-1/2}$, $u^2 = u_1^2 + u_2^2$, $\beta_1 = u_1/c$, and $\beta_2 = u_2/c$.

The connection between the two sets of rest frame coordinates, x' at time t and x'' at time $t + \delta t$, corresponding to the frames instantaneously co-moving with the particle in its accelerated motion, are given by,
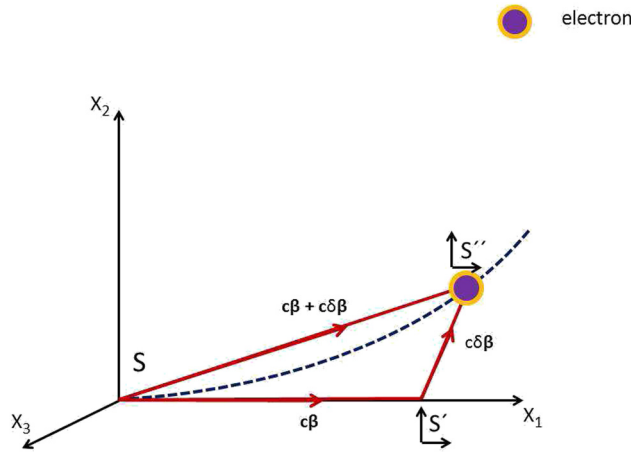

Figure A2: An object (electron) is in accelerated motion along a curvilinear path under the action of external forces. The moving frames S' and S'' represent successive rest frames of the object. Starting from the origin of the laboratory frame S, the velocity of the rest frame S' at time t is $\mathbf{v}(t) = c\beta$ and at time $t + \delta t$ the velocity of the rest frame S'' is $v(t + \delta t) = c\beta + c\delta\beta$. The resulting infinitesimal LT from S' to S'' consists of a boost and a rotation, indicating that the object acquires a precession at the Thomas angular velocity $\boldsymbol{\omega}_T$ of purely relativistic kinematical origin independent of other effects.

$$
\begin{aligned}
x' &= A_{\text{boost}}(\boldsymbol{\beta})x \\
x'' &= A_{\text{boost}}(\boldsymbol{\beta} + \boldsymbol{\delta\beta})x,
\end{aligned}
$$

where $\boldsymbol{\beta} = \mathbf{v}/c$ and $\boldsymbol{\beta} + \boldsymbol{\delta\beta} = \mathbf{u}/c = \mathbf{v}/c + \boldsymbol{\delta\beta}$, with the factor $\gamma_u = \gamma + \gamma^3 \beta \delta\beta_1$ to the first order in $\delta\beta$. The resulting infinitesimal transformation between S' and S'' is,

$$
x'' = A_{\text{LT}} x',
\tag{A3}
$$

where the transformation matrix,

$$
A_{\text{LT}} = A_{\text{boost}}(\boldsymbol{\beta} + \boldsymbol{\delta\beta})A_{\text{boost}}^{-1}(\boldsymbol{\beta}),
\tag{A4}
$$

is,

$$
A_{\text{LT}} =
\begin{pmatrix}
1 & -\gamma^2 \delta\beta_1 & -\gamma \delta\beta_2 & 0 \\
-\gamma^2 \delta\beta_1 & 1 & \dfrac{\gamma - 1}{\beta}\delta\beta_2 & 0 \\
-\gamma \delta\beta_2 & -\dfrac{\gamma - 1}{\beta}\delta\beta_2 & 1 & 0 \\
0 & 0 & 0 & 1
\end{pmatrix}.
\tag{A5}
$$

As shown by Jackson [30], the resulting infinitesimal Lorentz transformation (A3) consists of a boost with velocity $c\Delta\boldsymbol{\beta}$ and a rotation $\Delta\boldsymbol{\Omega}$ given by,

$$
\Delta\boldsymbol{\Omega} = \frac{\gamma - 1}{\beta^2}\boldsymbol{\beta} \times \boldsymbol{\delta\beta}.
\tag{A6}
$$

The rotation is highlighted by the two antisymmetric matrix elements $(A_{\text{LT}})_{23}$ and $(A_{\text{LT}})_{32}$ of A_{LT},

$$
A_{\text{LT}} =
\begin{pmatrix}
\cdots & \cdots & \cdots & \cdots \\
\cdots & \cdots & \dfrac{\gamma - 1}{\beta}\delta\beta_2 & \cdots \\
\cdots & -\dfrac{\gamma - 1}{\beta}\delta\beta_2 & \cdots & \cdots \\
\cdots & \cdots & \cdots & \cdots
\end{pmatrix},
\tag{A7}
$$

indicating the existence of a rotation of the electron rest frame S'' by $\Delta\Omega$ about the x_3 axis. Because of the spacetime symmetry of the LT in (A2), the parameter time depends on space, $t'' = t''(t, x)$ and $t' = t'(t, x)$. Therefore, through the matrix multiplication (A4), we can see that the time dependence on space, related to relative simultaneity, is essential for providing the resulting antisymmetric matrix elements $(A_{\text{LT}})_{23}$ and $(A_{\text{LT}})_{32}$ of A_{LT} shown in (A7).

A direct consequence of expression (A6) is the resulting Thomas precession acquired by the object at the angular velocity,

$$
\boldsymbol{\omega}_T = -\lim_{\delta t \to 0} \frac{\Delta\boldsymbol{\Omega}}{\delta t} = \frac{\gamma^2}{\gamma + 1}\frac{\mathbf{a} \times \mathbf{v}}{c^2}.
\tag{A8}
$$

Then, if the rotating object has a component of $\mathbf{a}$ perpendicular to $\mathbf{v}$, the object acquires a Thomas precession of purely kinematical origin, independent of other effects.

The LTA based on absolute simultaneity predict no Thomas precession

The LTs based on absolute simultaneity (LTA) between frame S and S'' are given by,

$$x_0'' = \gamma_u^{-1} x_0$$

$$x_1'' = x_1 + \frac{\gamma_u - 1}{\beta^2}(\beta_1 x_1 + \beta_2 x_2)\beta_1 - \gamma\beta_1 x_0$$

$$x_2'' = x_2 + \frac{\gamma_u - 1}{\beta^2}(\beta_1 x_1 + \beta_2 x_2)\beta_2 - \gamma\beta_2 x_0 \qquad (A9)$$

$$x_3'' = x_3,$$

which are the same as the LT in (A2), save for the fact that the time parameter does not depend on space (absolute simultaneity) and is given by $c\tau'' = x_0'' = \gamma_u^{-1} x_0$, being τ'' the proper time on the particle rest frame S''.

Obviously, the spacetime symmetry of the LT is different from that of the LTA and, therefore, for observables that depend on symmetry, different predictions may be expected from the two different transformations.

Following the procedure adopted earlier, we proceed by calculating the connection,

$$x'' = A_{\text{LTA}} \ x', \qquad (A10)$$

using the LTA (instead of the LT) and derive the corresponding matrix A_{LTA} (A14).

The transformations between frame S' and S are,

$$\begin{aligned} x_0' &= \gamma^{-1} x_0 \Rightarrow x_0 = \gamma x_0' \\ x_1' &= \gamma(x_1 - \beta x_0) \Rightarrow x_1 = \gamma^{-1} x_1' + \gamma\beta x_0' \\ x_2' &= x_2 \Rightarrow x_2 = x_2' \\ x_3' &= x_3 \Rightarrow x_3 = x_3'. \end{aligned} \qquad (A11)$$

After substituting x_0 and x_1 given by (A11) in expression (A9), the connection $x'' = A_{\text{LTA}} \ x'$ of (A10) to the first order in $\delta\beta$ is found to be,

$$x_0'' = \gamma_u^{-1} x_0 = \gamma_u^{-1}\gamma x_0'$$

$$x_1'' = -\gamma_u\beta_1\gamma x_0' + \left(1 + \frac{\gamma_u - 1}{\beta^2}\beta_1\beta_1\right)(\gamma^{-1} x_1' + \beta\gamma x_0')$$

$$\qquad + \frac{\gamma_u - 1}{\beta^2}\delta\beta_2\beta_1 x_2' \qquad (A12)$$

$$x_2'' = -\gamma\delta\beta_2\gamma x_0' + \frac{\gamma - 1}{\beta^2}\delta\beta_2\beta_1(\gamma^{-1} x_1' + \beta\gamma x_0') + x_2'$$

$$x_3'' = x_3.$$

For the matrix elements $(A_{\text{LTA}})_{23}$ and $(A_{\text{LTA}})_{32}$, we may take into account that the velocity of S'' relative to S is $\beta_1 = \beta + \delta\beta_1$ and $\beta_2 = \delta\beta_2$ and $\gamma_u \approx \gamma$ to the first order in $\delta\beta$. Then, (A12) becomes,

$$x_0'' = \gamma_u^{-1}\gamma x_0'$$

$$x_1'' = \gamma(\beta + \frac{\gamma_u - 1}{\beta^2}\beta\beta_1\beta_1 - \gamma_u\beta_1)x_0'$$

$$\qquad + (1 + \frac{\gamma_u - 1}{\beta^2}\beta_1\beta_1)\gamma^{-1} x_1' + \frac{\gamma - 1}{\beta}\delta\beta_2 x_2' \qquad (A13)$$

$$x_2'' = \gamma(\frac{\gamma - 1}{\beta}\delta\beta_2\beta_1 - \gamma\delta\beta_2)x_0' + \frac{\gamma - 1}{\gamma\beta}\delta\beta_2 x_1' + x_2'$$

$$x_3'' = x_3.$$

From the connection $x'' = A_{\text{LTA}} \ x'$ given by Eq. (A13), we find that the elements of the corresponding matrix A_{LTA} relevant to our case are,

$$A_{\text{LTA}} = \begin{pmatrix} \cdots & \cdots & \cdots & \cdots \\ \cdots & \cdots & \frac{\gamma - 1}{\beta}\delta\beta_2 & \cdots \\ \cdots & \frac{\gamma - 1}{\gamma\beta}\delta\beta_2 & \cdots & \cdots \\ \cdots & \cdots & \cdots & \cdots \end{pmatrix}, \qquad (A14)$$

indicating that both the matrix elements $(A_{\text{LTA}})_{23}$ and $(A_{\text{LTA}})_{32}$ are positive, not antisymmetric, and do not reflect the existence of a rotation about the x_3 axis, as it is the case for the corresponding elements of the matrix A_{LT} Eq. (A5) derived with the LT. In fact, the matrix elements $(A_{\text{LTA}})_{23}$ and $(A_{\text{LTA}})_{32}$ indicate a relative distortion of axes due to length contraction in the direction of motion, but no relative rotation about the x_3 axis.

In conclusion, standard special relativity predicts the existence of the Thomas precession, which is related to the spacetime symmetry properties of the LT based on relative simultaneity. Instead, the LTA, based on conservation of simultaneity, predicts that the Thomas precession does not exist. With the examples of the Thomas precession, the RLSE, and other phenomena [6–9], we may infer that the LTA are not in general physically equivalent to the LT. Hence, the two transformations – and absolute and relative simultaneity – cannot be interchanged arbitrarily.

A.3 Calculating with the Lorentz transformations the intervals $T_\Leftarrow$, $T_\Rightarrow$ and $\Delta T = T_\Leftarrow - T_\Rightarrow$ for the RLSE

A.3.1 Showing that, for $D > 2vL/c$ and C* on the same (upper or lower) contour section, in the RLSE the round-trip time interval $T_\Rightarrow$ for the counter-moving photon is independent of D and the same as in the standard linear Sagnac effect

With reference to Figures 1(b) and 2(a), we assume that the counter-moving photon is emitted by C* when $D > 2vL/c$,

so that C* is always on the lower track during the round-trip interval $T_\Rightarrow$. In this case, the contour is always moving at speed $+v$ relative to C*. Then, the photon moving at speed c reaches point B when $ct = (L - D)/\gamma + vt$, i.e., at,

$$t_1 = \frac{L - D}{\gamma(c - v)} = \frac{\gamma(L - D)(1 + v/c)}{c},$$

where we have used the relation $1/\gamma^2 = (1 - v/c)(1 + v/c) = 1 - v^2/c^2$.

Moving now on the upper track, the photon travels from B toward A and reaches A when $L/\gamma - ct = vt$ after the interval,

$$t_2 = \frac{L}{\gamma(c + v)} = \frac{\gamma L(1 - v/c)}{c}.$$

After reaching A, the photon starts moving on the lower track to return to C*. Since point A has been moving at speed v toward C* during the interval $t_1 + t_2$, the position of A relative to C* is now $D/\gamma - v(t_1 + t_2)$ and the photon reaches C* when $D/\gamma - v(t_1 + t_2) = ct$, after the interval,

$$\begin{aligned}
t_3 &= \frac{D}{\gamma c} - \frac{v}{c}(t_1 + t_2) \\
&= \frac{D}{\gamma c} - \frac{v\gamma}{c}\left[\frac{(L - D)(1 + v/c)}{c} + \frac{L(1 - v/c)}{c}\right] \\
&= \frac{\gamma D(1 - v^2/c^2)}{c} - \frac{v\gamma}{c}\frac{2L}{c} + \frac{v\gamma}{c}\frac{D(1 + v/c)}{c} \\
&= \frac{\gamma D(1 + v/c)}{c} - \frac{v\gamma}{c}\frac{2L}{c}.
\end{aligned}$$
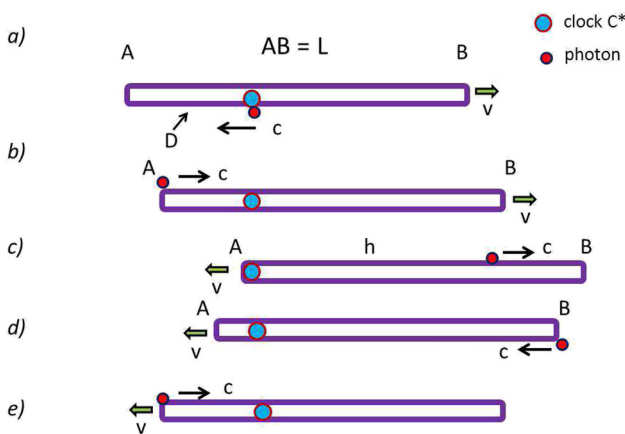
The resulting round-trip interval $T_\Rightarrow$ is,

Figure A3: Relative positions of photon and clock C* during light co-propagation in the round-trip interval $T_\Leftarrow$.

$$\begin{aligned}
T_\Rightarrow &= t_1 + t_2 + t_3 \\
&= \frac{\gamma(L - D)(1 + v/c)}{c} + \frac{\gamma L(1 - v/c)}{c} \\
&\quad + \frac{\gamma D(1 + v/c)}{c} - \frac{v\gamma}{c}\frac{2L}{c} \\
&= \frac{\gamma L(1 + v/c)}{c} + \frac{\gamma L(1 - v/c)}{c} - \frac{v\gamma}{c}\frac{2L}{c} \quad \text{(A15)}\\
&\quad - \frac{\gamma D(1 + v/c)}{c} + \frac{\gamma D(1 + v/c)}{c} \\
&= \frac{2\gamma L(1 - v/c)}{c} = \frac{2L}{\gamma(c + v)},
\end{aligned}$$

showing that, for $D > 2vL/c$, in the RLSE $T_\Rightarrow$, is D-independent and the same as that of the standard linear Sagnac effect in Eq. (1). The same conclusion holds for the round-trip $T_\Leftarrow$ of the co-propagating photon.

A.3.2 Showing that in general, for the RLSE the round trips intervals $T_\Leftarrow$ and $T_\Rightarrow$ depend on D. For two counter-propagating photons, the standard RLSE provides the same D-independent result ΔT of the standard linear Sagnac effect.

When during the round-trip interval T the device C* keeps on the same track (lower or upper contour section), there is no problem in deriving (as shown earlier) for $\Delta T = T_\Leftarrow - T_\Rightarrow$ the D-independent results (1)–(3), which are the same as those that can be found in literature. The calculations become quite complicated when the device C* passes, e.g., from the lower to the upper track and we wish to find results in general. Since in the variant S-RLSE, the round-trip $T_\Rightarrow$ has its maximum when the photon covers the maximum length $2L/\gamma$ (occurring when $D_0 = vL/(\gamma c)$), we consider here this special case and perform the calculations for deriving the round-trip $T_\Leftarrow$ of the co-moving photon and determine ΔT of (3). For the co-moving photon, we have first to find its position at $t_{\text{out}} = L/(\gamma c)$ when point A reaches C* and the rod changes the direction of motion. With reference to Figure A3(a), starting from C* and moving to the left at speed c toward point A, the photon reaches A when $-D_0 + vt = ct$, i.e.,

$$t_A = \frac{D_0}{c + v} = \frac{vL}{\gamma c(c + v)}.$$

After reaching A (Figure A3(b)), the photon moves to the upper track and, in the remaining interval, $\Delta t = t_{\text{out}} - t_A$ propagates on the upper track toward point B while the rod is still moving to the right at speed v. Then, since A is moving at speed v, after the interval Δt, the position of the photon relative to A is,

$$h = (c - v)\Delta t = (c - v)(t_{out} - t_A) = \frac{(c - v)L}{\gamma(c + v)},$$

as shown in Figure A3(c).

With the photon at distance h from A and the device C* coinciding with A and displaying the reading t_{out}, the contour changes direction of motion. Then, from h, the photon reaches B when, $h + ct = L/\gamma - vt$, i.e., after the interval,

$$t_2 = \frac{L/\gamma - h}{c + v} = \frac{1}{c + v}\left[\frac{L}{\gamma} - \frac{(c - v)L}{\gamma(c + v)}\right] = \frac{2vL}{\gamma(c + v)^2}$$

$$= \frac{2v\gamma L(1 - v/c)}{c(c + v)},$$

as indicated in Figure A3(d).

After reaching B on the upper track, the photon passes to the lower track and moves toward A, reaching it when $L/\gamma - ct = -vt$ at,

$$t_3 = \frac{L}{\gamma(c - v)},$$

as in shown Figure A3(e).

At this point, the photon at A goes to the upper track and starts moving toward C*. However, in the interval $t_2 + t_3$, point A has moved to the distance $v(t_2 + t_3)$ to the left of C*. Then, from A, the photon reaches C* when $ct = v(t_2 + t_3)$ after the interval,

$$t_4 = \frac{v(t_2 + t_3)}{c} = \frac{vL(2v(c - v) + (c + v)^2)}{\gamma c(c + v)^2(c - v)}$$

$$= \frac{v\gamma L(c^2 + 4vc - v^2)}{c(c + v)c^2}.$$

After some algebra, the resulting round-trip time interval for the co-propagating photon is found to be,

$$T_{\Leftarrow} = t_{out} + t_2 + t_3 + t_4$$

$$= \frac{L}{\gamma c} + \frac{2v\gamma L(1 - v/c)}{c(c + v)} + \frac{L}{\gamma(c - v)} \qquad \text{(A16)}$$

$$+ \frac{v\gamma L(c^2 + 4vc - v^2)}{c(c + v)c^2}.$$

The sum $t_{out} + t_3$ can be expressed as follows:

$$t_{out} + t_3 = \frac{L}{\gamma c} + \frac{L}{\gamma(c - v)} = \frac{2L}{\gamma c} - \frac{L}{\gamma c} + \frac{L}{\gamma(c - v)}$$

$$\text{(A17)}$$

$$= \frac{2L}{\gamma c} + \frac{vL}{\gamma c^2(1 - v/c)} = \frac{2L}{\gamma c} + \frac{\gamma vL(1 + v/c)}{c^2}.$$

By substituting Eq. (A17) in Eq. (A16), we find,

$$T_{\Leftarrow} = \frac{2L}{\gamma c} + \frac{\gamma vL(1 + v/c)}{c^2}$$

$$+ \frac{2v\gamma L(1 - v/c)}{c(c + v)} + \frac{v\gamma L(c^2 + 4vc - v^2)}{c(c + v)c^2} \qquad \text{(A18)}$$

$$= \frac{2L}{\gamma c} + \frac{\gamma vL(4c^2 + 4cv)}{c(c + v)c^2} = \frac{2L}{\gamma c} + \frac{4\gamma vL}{c^2},$$

and with $T_{\Rightarrow} = 2L/(\gamma c)$,

$$\Delta T = T_{\Leftarrow} - T_{\Rightarrow} = \frac{4\gamma vL}{c^2}$$

in agreement with the result of the standard linear Sagnac effect.